water

MDPI

Article

Quantifying the Impact of Coal Mining on Underground Water in Arid and Semi-Arid Area: A Case Study of the New Shanghai No. 1 Coal Mine, Ordos Basin, China

Yuguang Lyv [1,2], Wei Qiao [1,*], Weichi Chen [3,*], Xianggang Cheng [1], Mengnan Liu [1] and Yingjie Liu [1]

[1] Institute of Mine Water Hazards Prevention and Controlling Technology, School of Resources and Geosciences, China University of Mining and Technology, Xuzhou 221116, China; lvyg691208@126.com (Yuguang Lyv)
[2] Shandong Energy Xinwen Mining Inner Mongolia Energy Group Co., Ltd., Ordos 750336, China
[3] School of Transportation Engineering, Jiangsu Vocational Institute of Architectural Technology, Xuzhou 221116, China
* Correspondence: qiaowei@cumt.edu.cn (W.Q.); weichichen159@163.com (W.C.)

Abstract: The new Shanghai No. 1 Coal Mine is located in arid and semiarid area of northwest China, which is characterized by scarce rainfall, intense evaporation, and limited water resources. High-intensity coal mining has caused severe damage to groundwater resources. The Baotashan sandstone aquifer of the Jurassic system has abundant water resources, and they are stored in the floor strata of mining coal seams. This poses the risk of high-pressure build-up and water inrush hazards during the mining of coal. To avoid these, the Baotashan sandstone aquifer needs to be drained and depressurized, which can result in a huge waste of water resources. Thus, taking the New Shanghai No. 1 Coal Mine as the basis for the case study, the impact of coal mining on the underground water resources was quantified. Large-scale water release tests were performed under the shaft to determine the hydrogeological properties of the Baotashan sandstone aquifer and a three-dimensional numerical model of the groundwater system was established. The dynamic phenomenon of water drainage was simulated and the drained water discharge was predicted under the condition of safe mining.

Keywords: arid and semiarid area; quantitative assessment; groundwater; floor water inrush hazard; northwest China

check for updates

Citation: Lyv, Y.; Qiao, W.; Chen, W.; Cheng, X.; Liu, M.; Liu, Y. Quantifying the Impact of Coal Mining on Underground Water in Arid and Semi-Arid Area: A Case Study of the New Shanghai No. 1 Coal Mine, Ordos Basin, China. *Water* **2023**, *15*, 1765. https://doi.org/10.3390/w15091765

Academic Editors: Peiyue Li and Jianhua Wu

Received: 5 April 2023
Revised: 29 April 2023
Accepted: 1 May 2023
Published: 4 May 2023

1. Introduction

Water resource plays a vital role in industrial and agricultural development, ecological environmental protection, and vegetation growth [1–3], especially in arid and semiarid area of northwest China, where average annual precipitation is less than 400 mm and evaporation is greater than 2000 mm [4,5]. Underground water resources are extremely valuable in northwest China due to the scarcity of rivers and surface water bodies. On the contrary, this vast region is rich in oil, natural gas, and coal resources [6]. The coal reserves of northwest China accounted for approximately 73% of the national coal reserves [7], while coal output was estimated to be 1.83 billion tons in 2022, accounting for 58% of the total output of the country [8]. The resource strategy focused on the western regions and the energy structure of poor oil resources, limited gas resources, and abundant coal resources has driven up the mining intensity of northwest China [9,10].

Numerous studies have ascertained that coal mining has a negative impact on both surface and underground water resources, especially in arid and semiarid area [11–13]. Subsidence and surface cracks caused by high-intensity coal mining have changed the runoff generation and confluence within the catchment, resulting in decreased streamflow in the mining area [14–17]. The largest desert freshwater lake in China, Hongjiannao Lake, has seen a dramatic decline in its reservoir capacity and surface area due to the impact of coal mining [18]. Guo et al. (2019) quantified the effects of climate change, coal mining, and soil and water conservation on streamflow in the Kuye River Basin located in the arid and semiarid area of the Loess Plateau, China. They detected that the streamflow reduction induced by coal mining reached 29.88 mm, accounting for 54.24% of the total reduction [19]. Water-conducting fractures were found to have penetrated the aquifuges between the surface and the goaf causing massive water leakage, death of rivers, and eventually vegetation deterioration and ecological hazards [20,21]. Furthermore, the stress redistribution of overburden caused by underground coal mining led to the formation of caved zones and fractured zones in the roof strata, resulting in a dramatic increase in the permeability of the strata [22,23]. Thus, a complete groundwater drainage zone was formed in the roof aquifers [24]. Variations in the hydraulic characteristics of the strata such as the increase in the porosity, the opening of joints, and the separation of bedding planes resulted in the reduction of groundwater resources [25,26]. Furthermore, pre-drainage is adopted for the deep mining of the coal seams overlying the high-pressure confined aquifers to decrease the hydraulic pressure and prevent floor water inrush hazards [27–29]. However, the discharge of draining mine water from the roof and floor aquifers will cause the wastage of precious water resources and the contamination of the surface water systems which threatens human health [30–35].

Floor water inrush accidents have occurred frequently in the Permo-Carboniferous coal mining in north China, which caused massive casualties and economic loss [36]. Two main factors are responsible for these water hazards: high-pressure and ultrahigh-pressure of Ordovician limestone aquifers and the limited thickness of aquifuges underneath the mining coal seams [37]. Correspondingly, drainage and depressurization for the Ordovician limestone aquifers and grouting reinforcement for the limited-thickness aquifuges were proposed to prevent the floor water inrush [38]. Floor water inrush was a rare incidence in northwest China since the Ordovician limestone aquifers and Jurassic coal seams are separated by a considerable distance. However, on 25 November 2015, a severe floor water inrush hazard from the Jurassic Baotashan aquifer occurred in the New Shanghai No. 1 Coal Mine of Yinchuan city, Ningxia, northwest China [39]. The water inrush from the aquifer occurred from the floor strata during the advancement of deep roadway in the coal mine, wherein the initial water discharge was about 1500 m^3/h. The discharge of water inrush gradually increased with time. On 26 November 2015, the water discharge reached 3600 m^3/h, with the instantaneous discharge reaching 10,000 m^3/h, submerging the mine. To ensure safety during the mining activities, the Baotashen aquifer is planned to be drained and depressurized. This necessitates the quantification of the impact of coal mining on the Baotashan water resource, which is a valuable underground water resource in arid and semiarid areas.

2. Study Area

The New Shanghai No. 1 Coal Mine is located on the northwestern edge of the Mu Us Desert in the Ordos Basin (Figure 1), which has a semi-arid and semi-desert continental climate with annual precipitation of 150 mm and evaporation of 2770 mm. Due to the scarcity of surface water resources, industrial and agricultural water use is mainly from underground water sources. In recent years, the Ordos Basin has become the largest coal-producing region in China. It has coal reserves of 658.99 billion tons, which accounts for 38.8% of the total national reserves. Several national-level large coal development bases have been established, which have intensified the conflict over water resources.

The mining area of New Shanghai No. 1 Coal Mine is 26.6 km^2, with a length of 12.5 km and a width ranging from 2.0 to 3.5 km, approximately. The coal mine has 3.45 million tons of recoverable reserves and two mining levels are designed. The first level is at an altitude of +880 m, from which the coal seams of No. 2, No. 5, No. 8, No. 15, and No. 16 are mined. The second level is at an altitude of +700 m, and the coal seams of No. 18, No. 19, No. 20, and No. 21 are mined at this level. Combined mechanized mining and top-coal caving methods are adopted to excavate the coal seams. The coal seams are located in the strata of the Jurassic Yan'an formation. The lithology mainly consists of gray sandstone, gray black and black siltstone, and mudstone. The thickness of the Yan'an Formation layer ranges from 159 m to 345 m, with an average thickness of 288 m. The overlying strata of coal are in the order of Jurassic Zhiluo Formation, Cretaceous system, Paleogene system, and Quaternary system. The strata, lithology, and hydrogeological characteristics of overlying strata are described in detail in Figure 2.

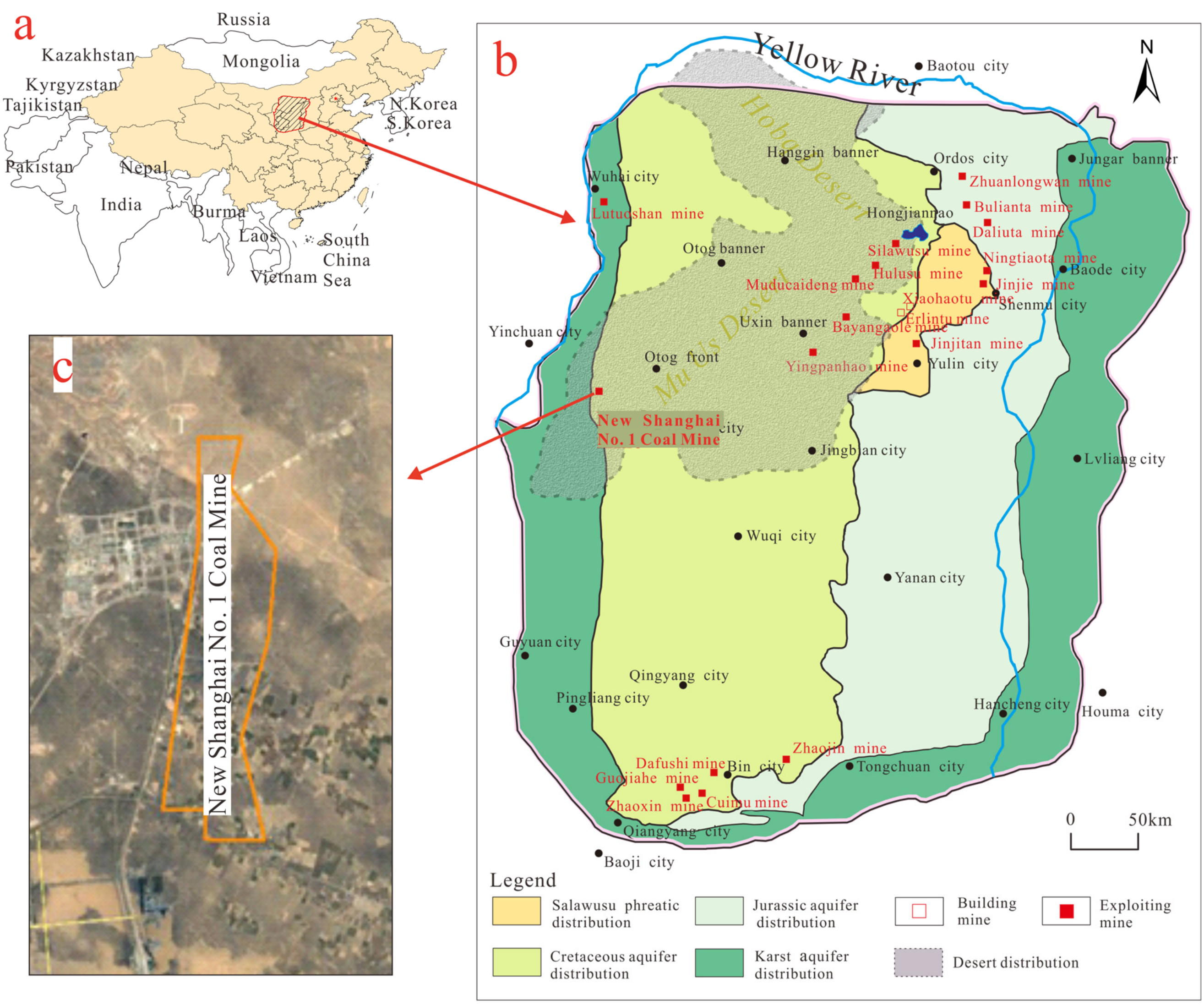

Figure 1. (**a**) Location of the study area in China; (**b**) water resources distribution of the Ordos Basin; (**c**) aerial photo of New Shanghai No. 1 Coal Mine.

At present, the No. 5, No. 8, and No. 15 coal seams, which are located in the upper part of the coal measure strata, have been mined. Penetrated by the water-conducted fractures, the groundwater stored in the sandstone aquifer of the Yan'an Formation and Zhiluo Formation is drained. Due to the low water abundance of the overlying strata, coal mining has little effect on groundwater resources. The No. 18 coal seam is planned to be mined in the next three years. The Jurassic Baotashan sandstone serving as the floor aquifer makes the coal mining highly probable of water inrush hazards.

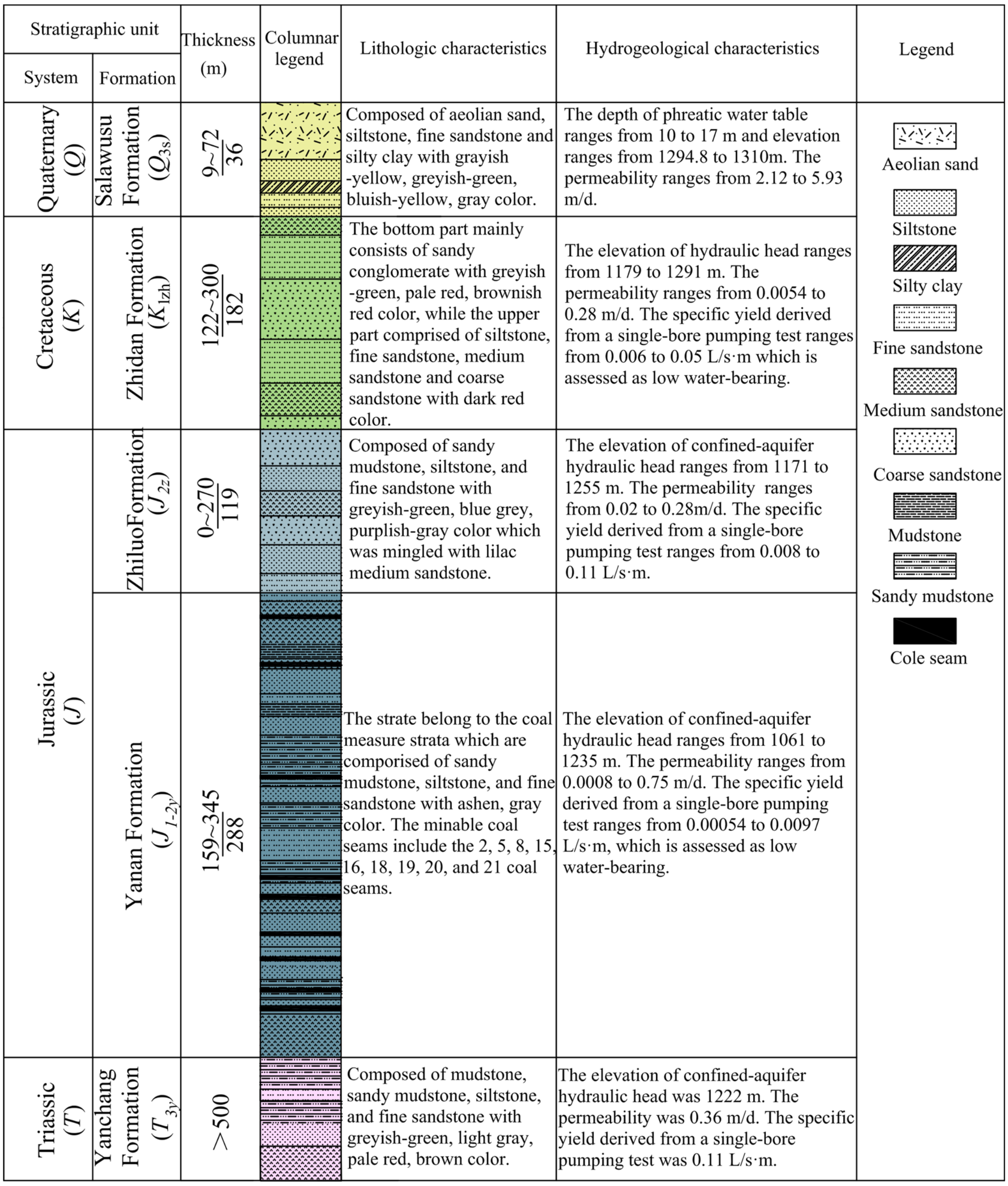

Figure 2. Stratigraphic column of the study area. The values in the thickness column refer to the thickness range and the average thickness.

3. Methodology

3.1. Water Release Test of Multiple Holes

Large-scale water release tests were conducted to investigate the hydrogeological property of the Baotashan sandstone aquifer and evaluate the impact of coal mining on groundwater resources. Four underground draining boreholes were drilled in the No. 8 coal mining roadway and were named as F1, F2, F3, and F4, respectively (Figure 3a). The spacing between adjacent draining holes was about 24 m. The diameter of the first-level drilling hole was 190 mm and the drilling depth was 16 m, where a sealing casing of 168 mm hole diameter and 6 mm wall thickness was installed. The second-level borehole was made by drilling a hole of 133 mm diameter to a depth of 1 m below the floor of the No. 21 coal seam in the Yan'an formation, where the sealing casing with a hole diameter of 108 mm and the wall thickness of 6 mm was installed. Finally, a borehole with a diameter of

85 mm was drilled to 5 m below the floor of the Baotashan sandstone aquifer. The structure of borehole is shown in Figure 3b.

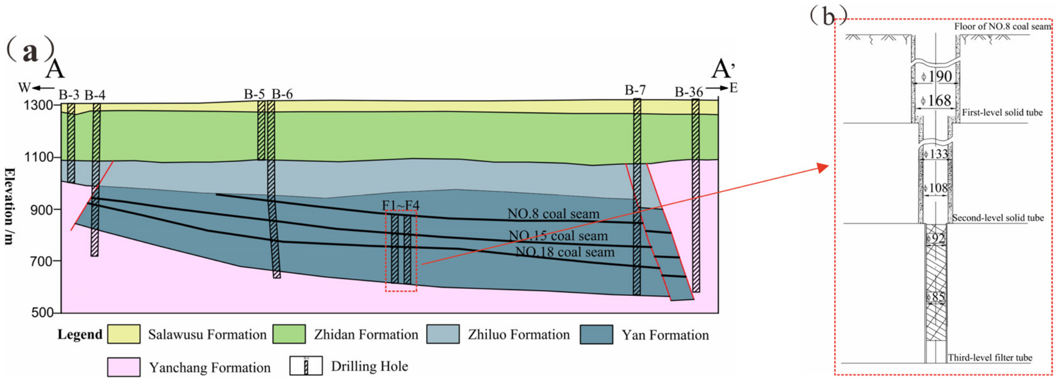

Figure 3. (**a**) cross-sectional location of water release holes from the Figure 4; (**b**) structure of drilling holes.

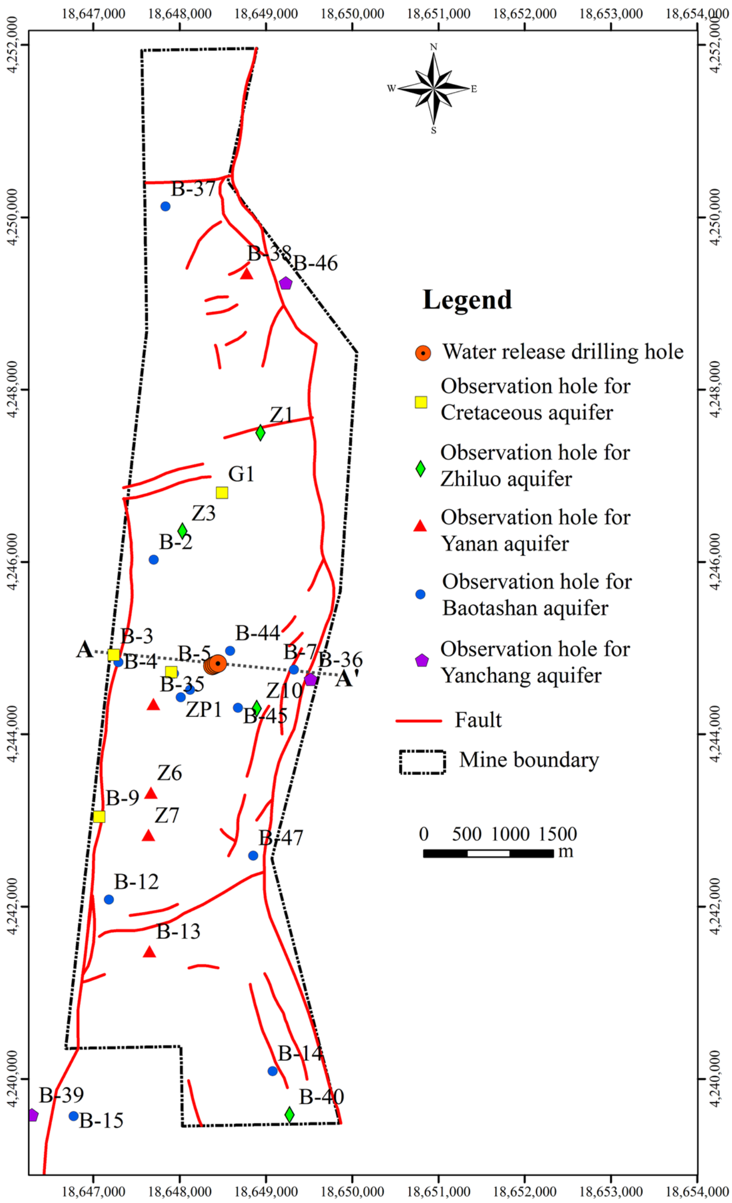

Figure 4. Layout of the water release test.

The water release test was divided into two parts: single-hole draining test and multi-hole draining test. In the single-hole draining test, the valve of the F2 hole was opened. The test started at 12 a.m. on 23 August 2019, and ended at 12 a.m. on 18 September 2019, lasting 624 h. During the test, the water discharge ranged from 180 m^3/h to 307 m^3/h, with an average of 237 m^3/h. In the multi-hole draining test, the valves of F1, F2, F3, and F4 holes were opened successively. On 8 October, the valve of the F2 hole was opened, which was referred to as the first draining stage. Then, the valve of F3 hole was opened on 12 October, which was named the second draining stage. Finally, the valves of F1 and F4 holes were opened on 16 October making the third draining stage. The multi-hole draining test ended on 6 November. The draining test lasted for 696 h and the hydraulic head recovery was 600 h. The average draining amounts of the first stage, second stage, and third stage were 206 m^3/h, 332 m^3/h, and 444 m^3/h, respectively.

Observation holes of hydraulic head to the Cretaceous aquifer, Zhiluo aquifer, Yan'an aquifer, Baotashan aquifer, and Triassic aquifer were used during the water release test of the Baotashan sandstone aquifer. There were four observation holes for the Cretaceous aquifer, namely G1, B-3, B-5, and B-9, four observation holes for the Zhiluo aquifer, namely holes Z1, Z3, Z10, and B-40, and six observation holes for the Yan'an Formation aquifer, namely holes Z6, Z7, B-13, B-24, B-35, and B-38. For the Baotashan sandstone aquifer, there were 11 observation holes, namely holes B-2, B-4, B-6, B-7, B-8, B-12, B-14, B-37, B-44, B-45, and B-47. The layout of the draining holes and observation holes are shown in Figure 4.

3.2. Numerical Simulation

To quantify the impact of coal mining on the groundwater resources of Baotashan sandstone, FEFLOW software was used to establish a three-dimensional (3D) numerical model of the groundwater system, as shown in Figure 5. Computational mesh densification was carried out in the area near the draining hole and the main faults in the well field. The model was divided on the plane into 18,420 calculation units and 9471 nodes. The model was divided vertically into seven layered structures, each representing a different aquifer.

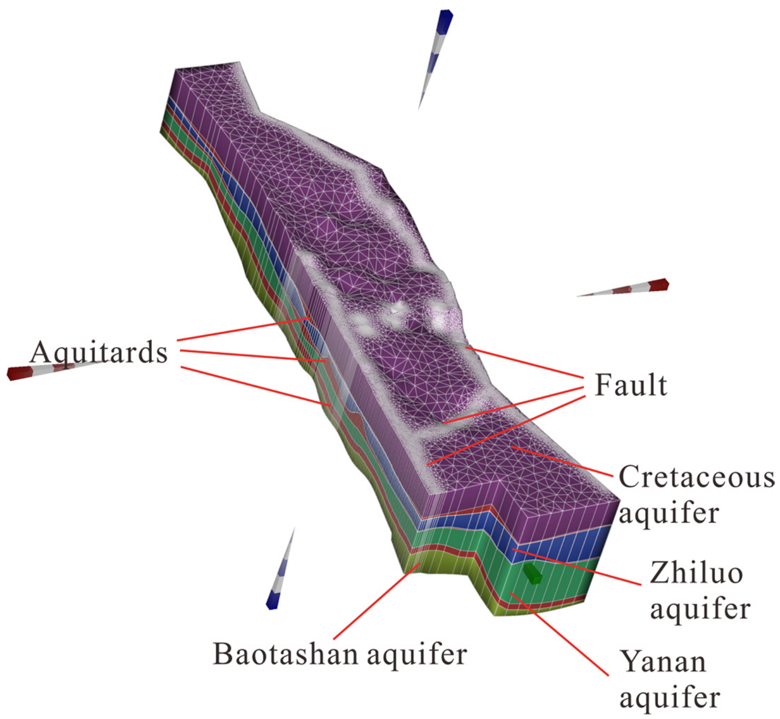

Figure 5. Three-dimensional (3D) model.

The first layer of the 3D numerical model was composed of the sandy mudstone and mudstone at the bottom of the Paleogene strata and the upper part of the Cretaceous strata, which blocks the hydraulic recharge of shallow water to the groundwater system. Thus, zero-flow boundary condition was assigned to the top boundary of the model. Similarly, zero-flow boundary condition was applied on the bottom boundary as well, since the seventh layer of the model was composed of the Baotashan sandstone aquifer, the floor of which consisted of mudstone of the Triassic strata.

Horizontally, the center fault segment of the western boundary was designated as the permeable boundary, while the southern and northern segments of the fault were generalized as impermeable boundaries. As illustrated in Figure 6a, the north fault segment of the eastern boundary was generalized as the permeable boundary, while the south segment was assigned as the impermeable boundary. The hydrogeological zoning of the Baotashan sandstone aquifer was divided into five zones according to its permeability and water-bearing capacity, as shown in Figure 6b. The parameters of zonings were inversely calculated during the fitting and verification of the numerical model.

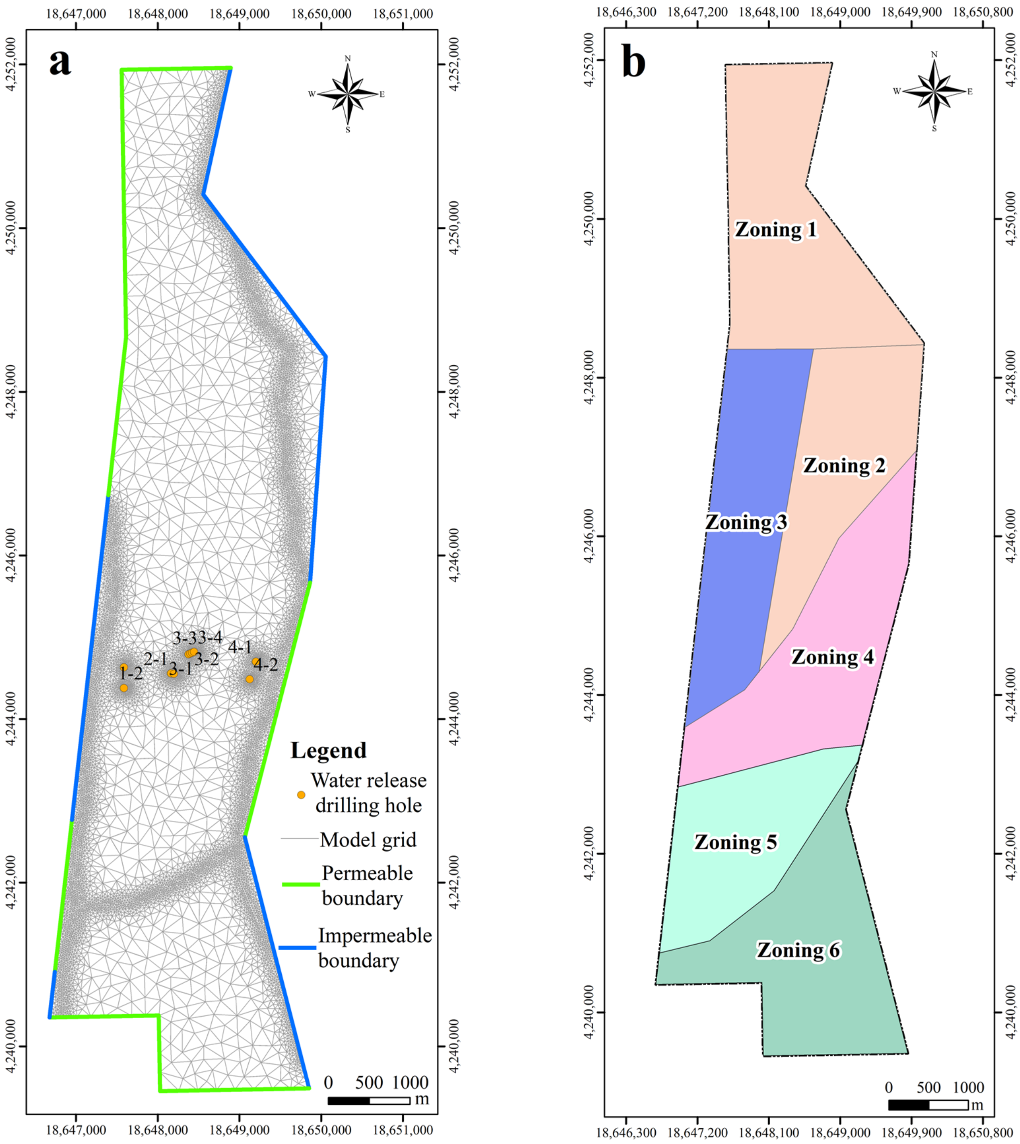

Figure 6. Numerical model generalization: (**a**) boundary generalization; (**b**) zoning of hydrogeological parameters.

4. Results

4.1. Hydrogeological Characteristics of the Baotashan Aquifer

The flow field of the natural, the single-hole draining test, and the multi-hole draining test are shown in Figure 7. The natural hydraulic head of the Baotashan sandstone aquifer ranges from 1184 m to 1228 m, with the lowest head occurring at the southwestern boundary of the well field. This indicates that the aquifer flows from the south and north of the well field to the southwest boundary. Figure 7b,c shows that the head drops for the single-hole draining test and the multi-hole draining test were more than 50 m and 100 m, respectively. This caused the depression-cone to develop in the middle of the draining holes. Additionally, the head contour distribution between observation holes B-12, B-47, and draining holes forms an extremely sparse area. It is analyzed that the predominant seepage zone is formed due to the existence of faults, which makes the area near observation holes B-12 quickly recharge to the draining area.

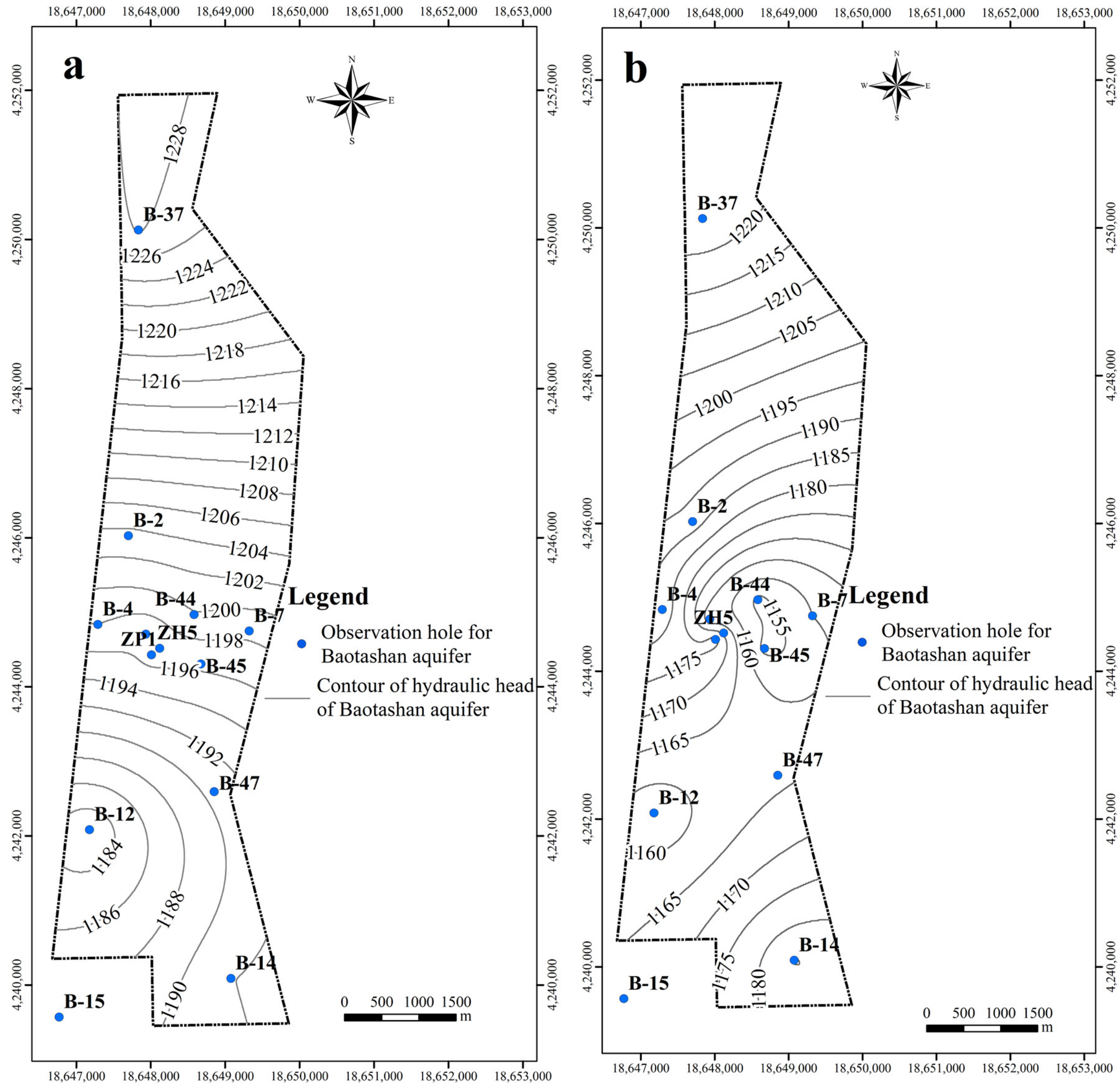

Figure 7. *Cont.*

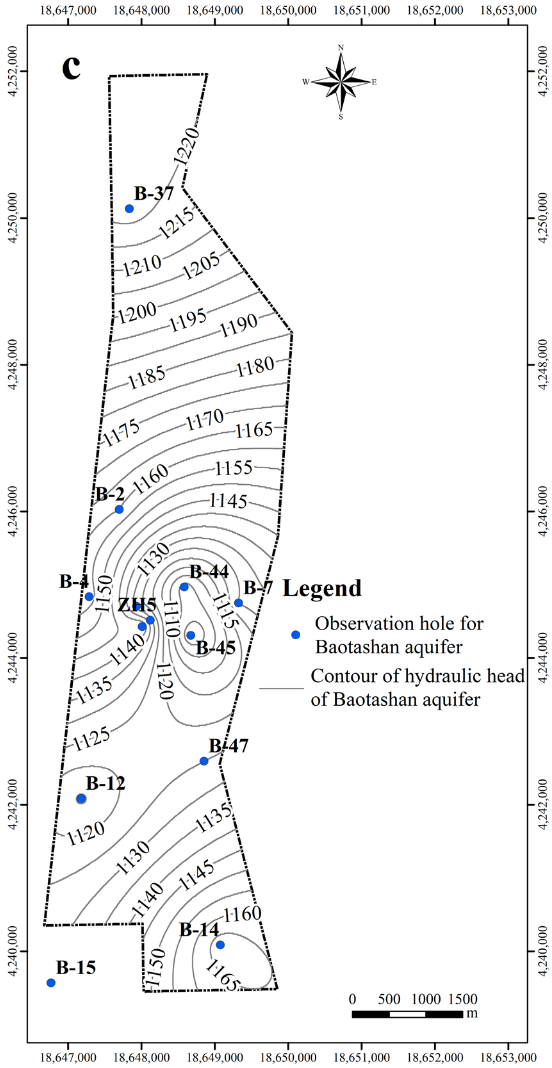

Figure 7. Variation of flow field during the water release tests: (**a**) before the water release tests; (**b**) single-hole water release tests; (**c**) multi-hole water release tests.

The permeability coefficient of the Baotashan sandstone aquifer is calculated based on the variation of water heads, as shown in Table 1. To accurately evaluate the water abundance of the aquifer, the single-hole unit inflow is calculated based on the previous pumping tests, which refers to the water inflow amount when the head is decreased a meter in the borehole during pumping tests. It is an important index for evaluating the degree of the water hazard in coal mines in China.

Table 1. Hydrogeological parameters of the Baotashan aquifer.

Borehole	Aquifer Thickness (m)	Water Level (m)	Permeability (m/d)	Unit Inflow (L/(s·m))
B-2	62.10	1200.03	0.3299	0.2048
B-4	127.10	1195.83	0.1057	0.1233
B-6	79.70	1183.862	0.4839	0.4669
B-7	53.50	1180.87	2.0247	0.9483
B-8	53.55	1187.241	1.7726	0.6783
B-12	56.85	1185.63	1.9688	1.0026
B-14	14.21	1184.609	0.288	0.0372
B37	56.35	1233.792	0.2541	0.1803
B44	81.00	1198.322	1.4290	1.5380
B45	58.98	1193.871	2.0603	0.9978
B47	42.18	1171.521	1.0955	0.4553

The permeability and unit inflow cloud maps of the Baotashan sandstone aquifer are shown in Figure 8. The permeability coefficient ranges from 0.1 m/d to 2.0 m/d and the high-permeability area is mainly caused by the tensile normal faults, which act as channels for water flow exchange.

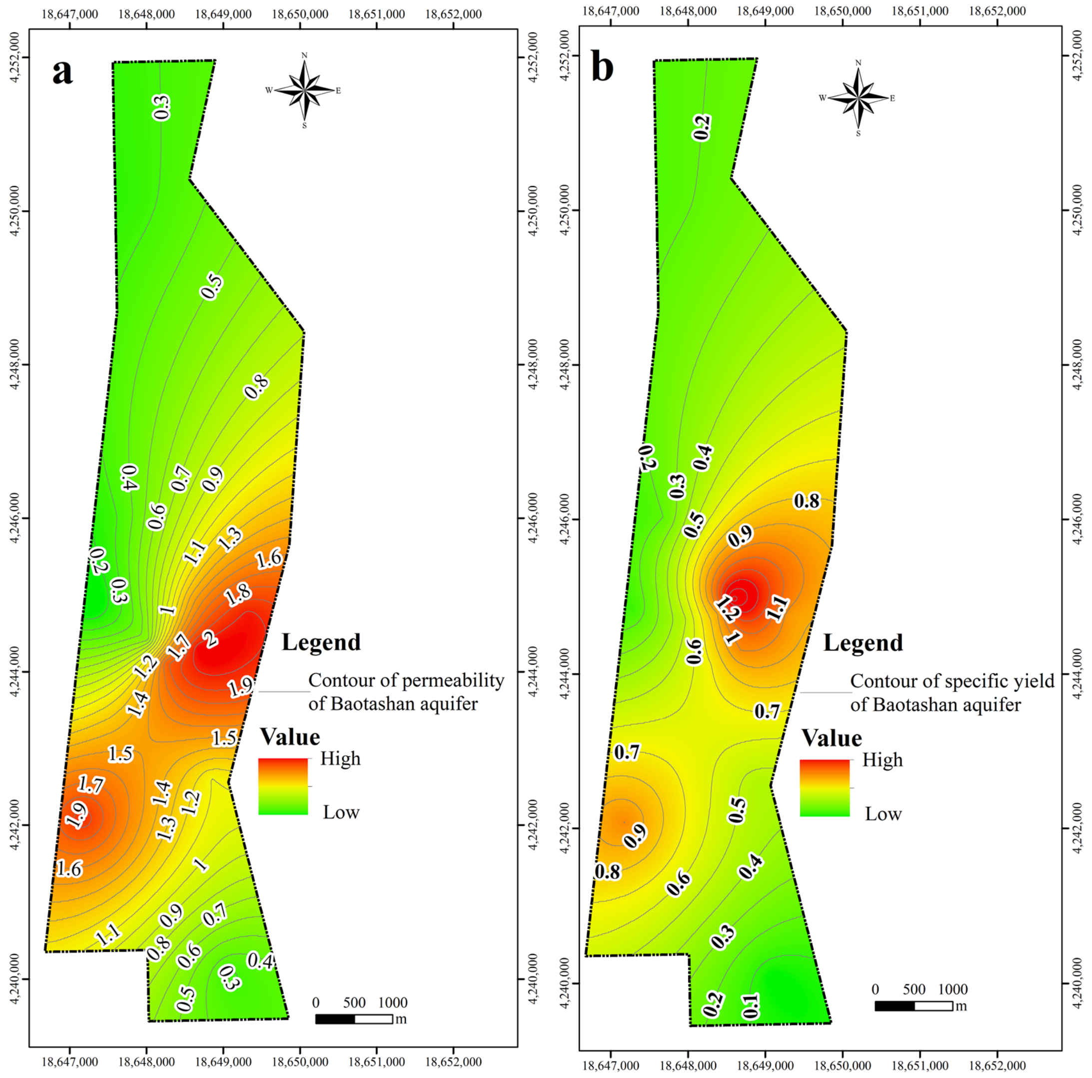

Figure 8. Hydrogeological parameters distribution of Baotashan aquifer: (**a**) permeability coefficient; (**b**) single-hole specific yield.

According to the classification standards of unit inflow in China, the majority of the areas near the Baotashan sandstone aquifer have medium water abundance, some local areas to the west and south have weak water abundance, and the area near the fault has strong water abundance, as shown in Figure 8b. Analyzing the data based on the permeability distribution, it is found that the area with high permeability also has good water abundance, suggesting that the water inrush amount of the Baotashan sandstone aquifer would be huge when the coal mining is carried out.

4.2. Influence on Water Resources of Baotashan Aquifer

4.2.1. Simulation Model Fitting

The comparison between the simulated and observed flow fields of the Baotashan aquifer is shown in Figure 9. It is difficult to effectively predict flow change using zoning parameters in faulted regions because the prevalent seepage channels resulted in the fast decrease of hydraulic head in local area. For example, in the area near the FD5 fault, the fitting error is about 2.46 m, indicating that the simulated head is higher than the observed head. Except for the area near the FD5 fault, the fitting of all the hydraulic heads is accurate.

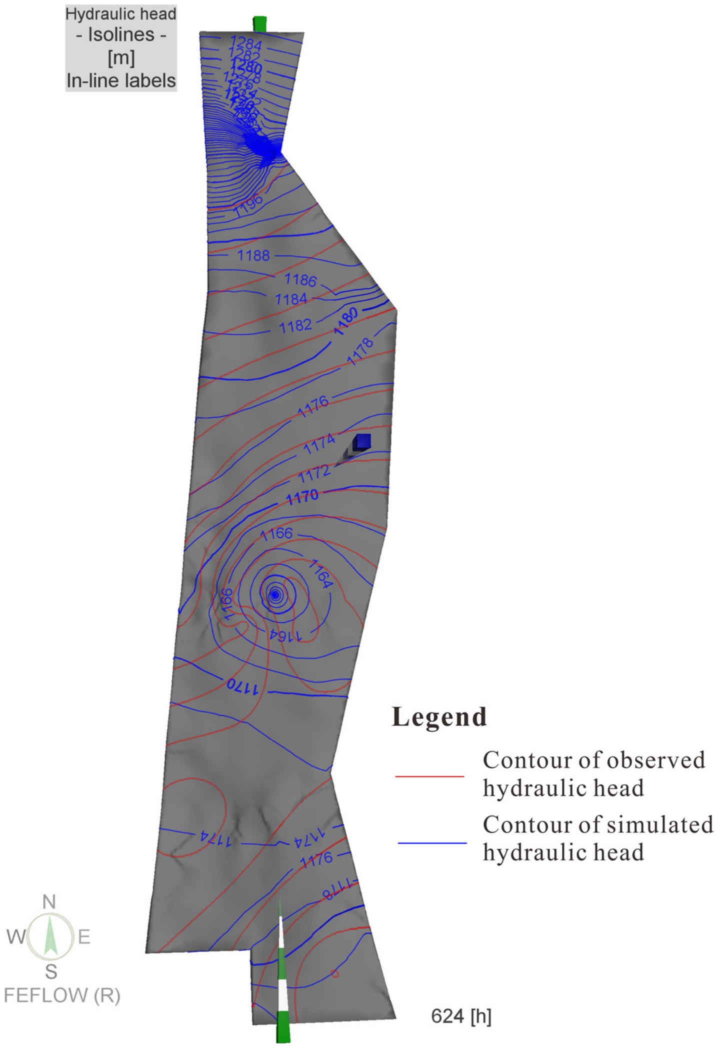

Figure 9. Fitting flow field of Baotashan aquifer between the observed and simulated hydraulic head.

Taking the hydrogeological parameters in Table 1 as initial parameters, the zoning parameters of the aquifer were inversely calculated, as shown in Table 2. The horizontal permeability coefficient of the Baotashan aquifer ranges from 0.67 m/d to 3.2 m/d, and the vertical permeability coefficient is found to be one-tenth of the horizontal permeability coefficient. The water-specific storage ranges from 1.5×10^{-7} m^{-1} to 1.3×10^{-6} m^{-1}.

Table 2. Parameter zoning of Baotashan sandstone aquifer.

Zone	Kx (m/d)	Ky (m/d)	Kz (m/d)	Ss (1/m)
Zone 1	1.25	1.25	0.12	2.1×10^{-7}
Zone 2	2.3	2.3	0.23	3.7×10^{-7}
Zone 3	0.67	0.67	0.06	1.5×10^{-7}
Zone 4	3.4	3.4	0.34	1.3×10^{-6}
Zone 5	2.9	2.9	0.29	7.8×10^{-6}
Zone 6	1.05	1.05	0.1	2.7×10^{-7}

4.2.2. Safe Mining Condition

The coefficient of water inrush has been widely used in coal mine production and plays an important role in evaluating the floor water inrush. The calculation formula for the water inrush coefficient is as follows:

$$T = \frac{p}{M} \tag{1}$$

where T is the water inrush coefficient (MPa/m), p is the water pressure (MPa), and M represents the thickness of the aquifuge floor (m).

According to the water inrush coefficient stipulated in China, the area with a water inrush coefficient below 0.06 MPa/m belongs to the safe mining zone when the impermeable floor is complete, whereas it is designated as a dangerous mining area when the water inrush coefficient is greater than 0.1 MPa/m. Under the latter condition, water inrush may occur during coal mining.

The hydraulic pressure distribution of the Baotashan aquifer was calculated, which ranges from 2.63 MPa to 7.06 MPa, with an average value of 4.72 MPa. The water inrush coefficient distribution of the Baotashan sandstone aquifer was obtained using the effective thickness of the impermeable floor and the hydraulic pressure, as shown in Figure 10. The water inrush coefficient of the Baotashan aquifer in most areas is found to be greater than 0.1 MPa/m. No specific area is found with a water inrush coefficient below 0.06 MPa/m. The water inrush coefficient of the Baotashan aquifer within the planned mining panel ranges from 0.08 Mpa/m to 0.51 MPa/m, indicating that there is a water inrush risk during coal mining. Thus, it is necessary to discharge water from the Baotashan aquifer to ensure safe mining.

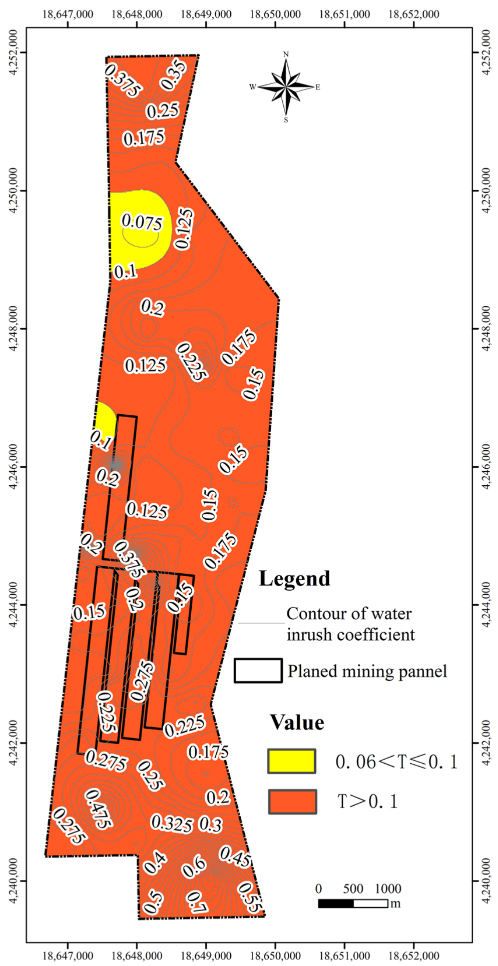

Figure 10. Distribution of water inrush coefficient of Baotashan aquifer.

4.2.3. Scheme of Water Drainage

Three additional draining fields with eight draining holes were arranged. The elevation of draining fields was 910, 880, and 750 m, respectively. Adding the previous four draining holes, a total of ten boreholes were arranged to release the water from the Baotashan aquifer. Since the new draining holes were spaced at a large distance from each other, the estimated drainage water amount of each hole was 3000 m^3/d. The estimated amount of the previous four draining holes was 2000 m^3/d. Thus, the total drainage water amount was 26,000 m^3/d. The numerical simulation was performed to simulate the dewatering scheme of the Baotashan aquifer.

Due to the varying elevation of each draining field, the draining holes would stop dewatering when the hydraulic head fell below the filed elevation. Therefore, initially, ten draining holes in four fields were functioning, and the draining water amount was 2.6×10^4 m^3/d. This was named the first draining stage. When the highest elevation surpassed the head, two holes were withdrawn. At this stage, eight boreholes in the remaining three draining fields were used to dewater the Baotashan aquifer, with an estimated water amount of 2×10^4 m^3/d. This stage was named the second draining stage. Finally, the remaining two draining fields and four holes were used to dewater the Baotashan aquifer, with an estimated amount of 1.2×10^4 m^3/d. The last stage was named the third draining stage.

As shown in Figure 11, the simulation results of the three draining stages reveal that the hydraulic pressure of the Baotashan aquifer satisfies the requirements of safe mining conditions after 241 days of large-scale drainage. The water inrush coefficient is less than 0.06 MPa/m in most areas, and the water inrush coefficient in most working faces of the No. 18 coal seams is less than 0.06 MPa/m, except for the local eastern areas.

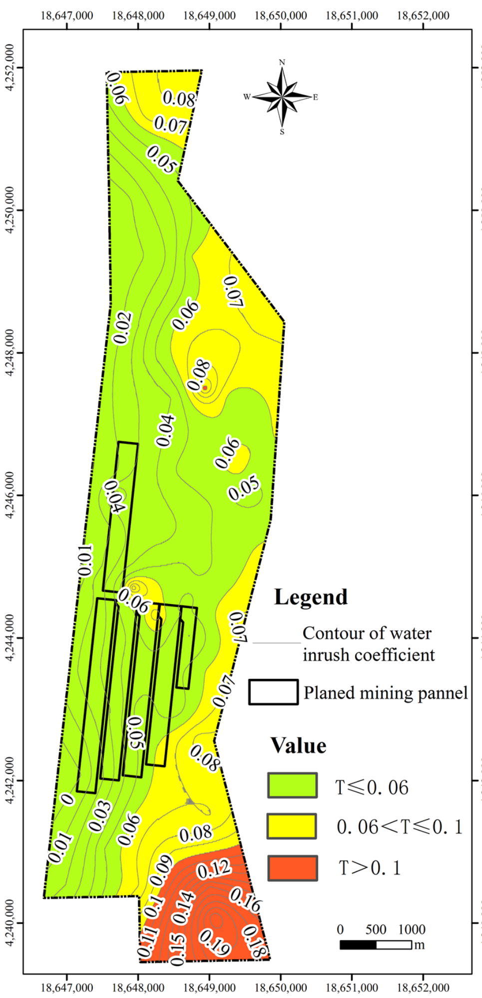

Figure 11. Distribution of water inrush coefficient of Baotashan aquifer after the draining depressurization.

The draining water amount of the Baotashan aquifer was calculated, as shown in Table 3. An amount of 4.314 million m^3 was released in 241 days, of which the elastic hydrostatic reserve of Baotashan sandstone was 367,600 m^3 and the boundary recharge was 3.9461 million m^3 accounting for 91.47% of the total water amount. In the first draining stage, the elastic water release capacity of Baotashan sandstone was 2991 m^3/d, accounting for 11.5% of the total amount of 26,000 m^3/d. Whereas, the water recharge amount was 23,009 m^3/d, accounting for 88.5% of the total amount. As the draining water advanced, the proportion of model static reserves in the total released water reduced progressively due to the expansion of the falling funnel.

Table 3. Simulated water balance statistics of Baotashan drainage water.

Stage	Draining Amount (m^3/d)	Time (d)	Static Storage (m^3/d)	Boundary Recharge (m^3/d)
First stage	26,000	73	2991 (11.5%)	23,009 (88.5%)
Second stage	20,000	50	1822 (9.12%)	18,177 (90.88%)
Third stage	12,000	118	495 (4.12)	11,505 (95.88%)
Total	431.4×10^4 m^3	241	36.76×10^4 m^3	394.61×10^4 m^3

5. Discussion

The Baotashan aquifer was drained to extract the No. 18 coal seam, wherein the water amount reached 4.31 million m^3, causing significant damage to groundwater in arid and semiarid areas. The fault created a major seepage channel to the west and south of the mining area. To reduce the impact of coal mining on the groundwater system, grouting was proposed to block the hydraulic recharge to the Baotashan aquifer. Distinguishing the grouting effects, the permeability coefficient of the fault was designed to be 2×10^{-2} m/d, 2×10^{-4} m/d, 2×10^{-6} m/d, and 2×10^{-8} m/d.

As shown in Table 4, when the permeability of the fault was designed as 2×10^{-2} m/d, the first, second, and third stages of the drainage took 70 days, 44 days, and 110 days, respectively, for completion, and the drainage water amount was 4.02 million m^3. Compared to the original scheme, the draining time was reduced by 19 days and the amount was reduced by 294,000 m^3. The period of water drainage was gradually shortened and the volume of water was lowered as the grouting effect was progressively improved. When the permeability of fault after grouting was designed as 2×10^{-6} m/d, the drainage time was 195 days and the drainage water was 3.502 million m^3. Compared to the original scheme, the drainage time was reduced by 46 d and the drainage amount was reduced by 812,000 m^3. The grouting of the fault prevented the hydraulic recharge of the southern region of the well field of the Baotashan aquifer. This led to the gradual reduction of the boundary recharge with the enhancement of the grouting effect.

Table 4. Optimization for the Baotashan aquifer drainage simulation.

Grouting Effect of Fault (m/d)	Stage 1 (d)	Stage 2 (d)	Stage 3 (d)	Discharge Water ($\times 10^4$ m^3)	Static Reserves of Model ($\times 10^4$ m^3)	Boundary Supply ($\times 10^4$ m^3)
No grouting	73	50	118	431.4	36.76	394.61
2×10^{-2}	70	44	110	402	38.53	363.47
2×10^{-4}	68	41	106	386	41.32	344.68
2×10^{-6}	63	35	97	350.2	45.19	305.01
2×10^{-8}	63	35	95	347.8	45.57	302.23

6. Conclusions

High-intensity coal mining has a profound impact on groundwater resources, especially in arid and semi-arid parts of western China, with there is a scarcity of rainfall and evaporation is intense. Thus, to evaluate the influence of No. 18 coal seam mining on the groundwater water resources in New Shanghai No. 1 Coal Mine, a series of large-scale drainage tests were carried out on the Baotashan aquifer to obtain its hydrogeological parameters. Based on the field data, a 3D numerical model was established. On the premise of safe mining, the influence of coal mining on groundwater resources was quantitatively evaluated. The following conclusions were derived:

According to the variation of the flow field of the Baotashan aquifer, the southwest boundary of the well field acted as the drainage boundary, and the north and south of the well field were recharge boundaries. The permeability coefficient of the Baotashan sandstone aquifer ranged from 0.1 to 2.0 m/d, and the permeability coefficient in the central region of the well field was found to be greater than that in the south and north regions. The working faces planned for mining were located in an area with a high permeability coefficient. The water abundance of most areas of the Baotashan aquifer was found to be in the medium-rich water abundance category.

The fitting error between the calculated water level and the water level obtained from the observation hole B-12 was relatively large, about 2.46 m. The water inrush coefficient of the Baotashan aquifer was further calculated. The water inrush coefficient of the No. 18 coal seam floor was between 0.08 Mpa/m and 0.51 MPa/m, indicating that there was a risk of floor water inrush during the mining. Therefore, water from the Baotashan aquifer had to be released before coal mining. The simulation results showed that the water pressure of the Baotashan aquifer meets the safe mining requirements after 241 days of large-scale drainage. The total amount of water discharged was about 4.314 million m^3. Subsequently, grouting of the fault was suggested to reduce the influence of groundwater resources. The drainage water steadily decreased as the grouting effect was improved. When the permeability of the fault was designed as 2×10^{-6} m/d, the drainage time and water amount were 195 days and 3.502 million m^3, respectively. Furthermore, the drainage time was 46 days less than the original scheme, and the amount was reduced by 812,000 m^3.

Author Contributions: Methodology, Y.L. (Yuguang Lyv) and W.Q.; simulation, W.C.; validation, W.C. and W.Q.; formal analysis, W.C.; investigation and resources, Y.L. (Yuguang Lyv); writing—original draft preparation, Y.L. (Yingjie Liu); writing—review and editing, X.C. and M.L.; supervision, W.Q.; project administration, Y.L. (Yuguang Lyv); funding acquisition, W.Q. All authors have read and agreed to the published version of the manuscript.

Funding: This research was funded by [National Natural Science Foundation] grant number [41772302] and funded by [National Natural Science Foundation] grant number [42007240]. The APC was funded by [National Natural Science Foundation] grant number [41772302].

Institutional Review Board Statement: Not applicable.

Informed Consent Statement: Not applicable.

Data Availability Statement: Data used in this study will be available upon request from the first author.

Conflicts of Interest: The authors declare no conflict of interest.

References

1. Afzal, M.; Battilani, A.; Solimando, D.; Ragab, R. Improving water resources management using different irrigation strategies and water qualities: Field and modelling study. *Agr. Water Manag.* **2016**, *176*, 40–54. [CrossRef]
2. Islam, M.B.; Firoz, A.B.M.; Foglia, L.; Marandi, A.; Khan, A.R.; Schüth, C.; Ribbe, L. A regional groundwater-flow model for sustainable groundwater-resource management in the south Asian megacity of Dhaka, Bangladesh. *Hydrogeol. J.* **2017**, *25*, 617–637. [CrossRef]
3. Kotir, J.H.; Smith, C.; Brown, G.; Marshall, N.; Johnstone, R. A system dynamics simulation model for sustainable water resources management and agricultural development in the Volta River Basin, Ghana. *Sci. Total Environ.* **2016**, *573*, 444–457. [CrossRef] [PubMed]
4. Liu, S.L.; Li, W.P.; Qiao, W.; Wang, Q.Q.; Hu, Y.B.; Wang, Z.K. Effect of natural conditions and mining activities on vegetation variations in arid and semiarid mining regions. *Ecol. Indic.* **2019**, *103*, 331–345. [CrossRef]
5. Zhang, D.S.; Li, W.P.; Lai, X.P.; Fan, G.W.; Liu, W.Q. Development on basic theory of water protection during coal mining in northwest of China. *J. China Coal Soc.* **2016**, *42*, 36–43. (In Chinese)
6. Wang, S.M. *Coal Accumulating and Coal Resource Evaluation of Ordos Basin*; China Coal Industry Publication House: Beijing, China, 1996. (In Chinese)

7. Qiao, W.; Li, W.P.; Li, T.; Chang, J.Y.; Wang, Q.Q. Effects of coal mining on shallow water resources in semiarid regions: A case study in the Shennan mining area, Shaanxi, China. *Mine Water Environ.* **2017**, *36*, 104–113. [CrossRef]
8. China National Energy Administration. Available online: http://www.nea.gov.cn (accessed on 6 March 2023).
9. Wang, J.H.; Kang, H.P.; Liu, J.Z.; Chen, P.P.; Fan, Z.Z.; Yuan, W.M.; Liu, Y.P. Layout strategic research of green coal resource development in China. *J. China Univ. Min. Technol.* **2018**, *47*, 15–20. (In Chinese)
10. Yuan, L.; Zhang, N.; Kan, J.G.; Wang, Y. The concept, model and reserve forecast of green coal resources in China. *J. China Univ. Min. Technol.* **2018**, *47*, 1–8. (In Chinese)
11. Booth, C.J.; Spande, E.D.; Pattee, C.T.; Miller, J.D.; Bertsch, L.P. Positive and negative impacts of longwall mine subsidence on a sandstone aquifer. *Environ. Geol.* **1997**, *34*, 223–233. [CrossRef]
12. Bruns, D.A. Macroinvertebrate response to land cover, habitat, and water chemistry in a mining-impacted river ecosystem: A GIS watershed analysis. *Aquati. Sci.* **2005**, *67*, 403–423. [CrossRef]
13. Candeias, C.; Ávila, P.F.; Ferreira, S.E.; Paulo, J.T. Integrated approach to assess the environmental impact of mining activities: Estimation of the spatial distribution of soil contamination (Panasqueira mining area, central Portugal). *Environ. Monit. Assess.* **2015**, *187*, 135–158. [CrossRef] [PubMed]
14. Chiew, F.H.S.; Fu, G.B.; Post, D.A.; Zhang, Y.Q.; Wang, B.; Viney, N.R. Impact of coal resource development on streamflow characteristics: Influence of climate variability and climate change. *Water* **2018**, *10*, 1161. [CrossRef]
15. Koch, H.; Kaltofen, M.; Grünewald, U. Scenarios of water resources management in the Lower Lusatian mining district, Germany. *Ecol. Eng.* **2005**, *24*, 49–57. [CrossRef]
16. Raghavendra, N.S.; Deka, P.C. Sustainable development and management of ground water resources in mining affected area: A review. *Procedia Earth Planet. Sci.* **2015**, *11*, 598–604. [CrossRef]
17. Sosa1, M.; Zwarteveen, M. The institutional regulation of the sustainability of water resources within mining contexts: Accountability and plurality. *Curr. Opin. Environ. Sustain.* **2014**, *11*, 19–25. [CrossRef]
18. Yue, H.; Liu, Y. Water balance and influence mechanism analysis: A case study of Hongjiannao Lake, China. *Environ. Monit. Assess.* **2021**, *193*, 219–228. [CrossRef] [PubMed]
19. Guo, Q.L.; Han, Y.Y.; Yang, Y.S.; Fu, G.B.; Li, J.L. Quantifying the Impacts of Climate Change, Coal Mining and Soil and Water Conservation on Streamflow in a Coal Mining Concentrated Watershed on the Loess Plateau, China. *Water* **2019**, *11*, 1054. [CrossRef]
20. Cooper, D.J.; Sanderson, J.S.; Stannard, D.I.; Groeneveld, D.P. Effects of long-term water table drawdown on evapotranspiration and vegetation in an arid region phreatophyte community. *J. Hydrol.* **2006**, *325*, 21–34. [CrossRef]
21. Newman, C.; Agioutantis, Z.; Leon, G. Assessment of potential impacts to surface and subsurface water bodies due to longwall mining. *Int. J. Min. Sci. Technol.* **2017**, *27*, 57–64. [CrossRef]
22. Adhikary, D.P.; Guo, H. Modelling of longwall mining-induced strata permeability change. *Rock Mech. Rock Eng.* **2015**, *48*, 345–359. [CrossRef]
23. Tammetta, P. Estimation of the change in hydraulic conductivity above mined longwall panels. *Ground Water* **2015**, *53*, 122–129. [CrossRef] [PubMed]
24. Booth, C.J. The effects of longwall coal mining on overlying aquifers. *Geol. Soc. Spec. Publ.* **2002**, *198*, 17–45. [CrossRef]
25. Chen, W.C.; Li, W.P.; He, J.H.; Qiao, W.; Wang, Q.Q.; Yang, R.Y. Impact of mining-induced bed separation space on Cretaceous aquifer: A case study of Yingpanhao coal mine, Ordos Basin, China. *Hydrogeo. J.* **2022**, *30*, 691–706. [CrossRef]
26. Fan, K.F.; He, J.H.; Li, W.P.; Chen, W.C. Dynamic evolution and identification of bed separation in overburden during coal mining. Rock Mech. *Rock Eng.* **2022**, *55*, 4015–4030. [CrossRef]
27. Hu, Y.B.; Li, W.P.; Wang, Q.Q.; Liu, S.L.; Wang, Z.K. Evaluation of water inrush risk from coal seam floors with an AHP-EWM algorithm and GIS. *Environ. Earth Sci.* **2019**, *78*, 290–305. [CrossRef]
28. Li, W.P.; Liu, Y.; Qiao, W.; Zhao, C.X.; Yang, D.D.; Guo, Q.C. An improved vulnerability assessment model for floor water bursting from a confined aquifer based on the water inrush coefficient method. *Mine Water Environ.* **2018**, *37*, 196–204. [CrossRef]
29. Wu, Q.; Zhao, D.K.; Wang, Y.; Shen, J.J.; Liu, H.L. Method for assessing coal-floor water-inrush risk based on the variable weight model and unascertained measure theory. *Hydrogeol. J.* **2017**, *25*, 2089–2104. [CrossRef]
30. Singh, R.; Venkatesh, A.S.; Syed, T.H.; Reddy, A.G.S.; Kumar, M.; Kurakalva, R.M. Assessment of potentially toxic trace elements contamination in groundwater resources of the coal mining area of the Korba coalfield, central India. *Environ. Earth Sci.* **2017**, *76*, 566–573. [CrossRef]
31. Wessman, H.; Salmi, O.; Kohl, J.; Kinnunen, P.; Saarivuori, E.; Mroueh, U. Water and society: Mutual challenges for eco-efficient and socially acceptable mining in Finland. *J. Clean Prod.* **2014**, *84*, 289–298. [CrossRef]
32. Zipper, C.E.; Donovan, P.F.; Jones, J.W.; Li, J.; Price, J.E.; Stewart, R.E. Spatial and temporal relationships among watershed mining, water quality, and freshwater mussel status in an eastern USA river. *Sci. Total. Environ.* **2016**, *541*, 603–615. [CrossRef]
33. Howladar, M.F.; Deb, P.K.; Muzemder, A.S.H. Monitoring the underground roadway water quantity and quality for irrigation use around the Barapukuria Coal Mining Industry, Dinajpur, Bangladesh. *Groundw. Sustain Dev.* **2017**, *4*, 23–34. [CrossRef]
34. Guo, W.; Li, P.; Du, Q.; Zhou, Y.; Xu, D.; Zhang, Z. Hydrogeochemical Processes Regulating the Groundwater Geochemistry and Human Health Risk of Groundwater in the Rural Areas of the Wei River Basin, China. *Expo. Health* **2023**, *4*, 1–16. [CrossRef]

35. Yang, Y.; Li, P.; Elumalai, V.; Ning, J.; Xu, F.; Mu, D. Groundwater Quality Assessment Using EWQI With Updated Water Quality Classification Criteria: A Case Study in and Around Zhouzhi County, Guanzhong Basin (China). *Expo. Health* **2022**, *8*, 1–16. [CrossRef]
36. Sun, W.; Zhou, W.; Jiao, J. Hydrogeological classification and water inrush accidents in China's coal mines. *Mine Water Environ.* **2016**, *35*, 214–220. [CrossRef]
37. Yin, S.X.; Zhang, J.; Liu, D. A study of mine water inrushes by measurements of in situ stress and rock failures. *Nat. Hazards.* **2015**, *79*, 1961–1979. [CrossRef]
38. Chen, W.C.; Li, W.P.; Qiao, W.; Li, L.F. Beneficial Use of Deep Ordovician Limestone Water from Mine Safety Dewatering at the Xinglongzhuang Coal Mine, North China. *Mine Water Environ.* **2020**, *39*, 42–56. [CrossRef]
39. Zhao, B.F.; Lv, Y.G. Research on characteristics and prevention and control technology of sandstone water disaster in coal seam floor in Jurassic coalfield. *China Coal.* **2021**, *47*, 56–63. (In Chinese)